Position Error Modeling for Automated Construction Manipulators

Yong-Kwon Cho[1]; Carl T. Haas[2]; S. V. Sreenivasan[3]; and Katherine Liapi[4]

Abstract: Hydraulically actuated construction equipment is rapidly being retrofitted with robotic control capabilities by several major manufacturers. However, position control errors caused by several factors are significant in these types of construction equipment. Errors are amplified if the manipulator and its operator must measure and locate objects in the equipment's fixed reference frame. Both mechanistic and statistical approaches to correcting position errors are possible. A statistical approach is reported here that is validated based on experiments with a computer-controlled large-scale manipulator (LSM). The LSM is sufficiently representative of several types of construction equipment to be able to serve as a general test bed. In the regression analysis, three factors which are measurable in real time: distance, hydraulic pressure, and payload, were varied to determine their influence on position errors in the LSM. It was shown that with an integrated multivariable regression model, about 30% of the mean positioning error of the LSM can be reduced without the use of fixed external reference systems. The model can be implemented as simple, real-time regression equations.

DOI: 10.1061/(ASCE)0733-9364(2004)130:1(50)

CE Database subject headings: Construction industry; Automation; Models; Errors; Sensors; Kinematics; Regression analysis.

Introduction

Positioning materials and equipment accurately at a construction site is a critical process (Huang and Bernold 1997). A recent trend toward greater automation of hydraulically actuated construction equipment such as dozers, graders, and excavators equipped with various position sensors reflects a movement in the construction industry towards improving productivity, efficiency, and safety through automation (Singh 1997). The reduction of the cumulative position error caused by backlash, deflection, sensor error, and other factors, however, still remains as one of the key issues in autonomous or semiautonomous construction equipment operation.

The information from sensors must be sufficient and accurate enough to determine the kinematic state of the equipment. In the area of automation and robotics, sensors have long been used in controlled conditions to solve the many difficult problems arising from the interaction of remotely operated manipulators with their work environments. In field applications, however, unanticipated problems sometimes emerge relating to the sensor, the robot, the integration of their respective systems, and the environment (Papanikolopoulos and Smith 1998). Further, large scale construction equipment, particularly the ones actuated hydraulically, possess lower end-point positioning accuracy than electrically actuated robotic devices used in controlled environments.

Understanding the causes and propagation of errors in automated construction equipment is very important for precise operation in a field environment. Large manipulators such as forklifts, excavators, and the large-scale manipulator (LSM) on a crane (Fig. 1) pose particularly difficult equipment control problems. Much of the manipulator error is due to accumulated feedback errors of the rotary and prismatic joint sensors, and lost actuator motion due to backlash. Working conditions such as variations in hydraulic pressure supply and presence of large payloads influence the error attributes as well. Kinematic and dynamic states are also an influence. The measured error attributes can be analyzed and applied to each coordinate computation as simply expressed in the following equation:

$$\text{Total error} = \text{Desired manipulator end-effector position} - \text{Actual manipulator end-effector position} \tag{1}$$

Most errors arising from the operation of the manipulator are considered random errors. Random errors, so-called accidental errors, are unpredictable in regard to their inconsistent results. Sources of these errors include: inertia, friction, vibration, orientation, and mass distribution which make it extremely difficult for a manipulator to achieve the exact desired output.

While it may be theoretically possible to derive a mechanistic model of all error sources and their interdependence, it is currently computationally untenable to use such a model for real time manipulator control. Instead, the impact of error sources can be treated as a statistical problem. Position error of an economically sensor equipped manipulator can be reduced by providing the correction factors resulting from statistical analysis of a well constructed experimental program. The results can be organized into statistical equations with correction factors for real-time

[1] Assistant Professor, Dept. of Industrial Studies, Univ. of Wisconsin, Platteville, WI 53818 (corresponding author). E-mail: choyo@uwplatt.edu

[2] Professor, Dept. of Civil Engineering, The Univ. of Texas at Austin, TX 78712. E-mail: haas@mail.utexas.edu

[3] Associate Professor, Dept. of Mechanical Engineering, The Univ. of Texas, Austin, TX 78712. E-mail: sv.sreeni@mail.utexas.edu

[4] Assistant Professor, Dept. of Civil Engineering, The Univ. of Texas at Austin, TX 78712. E-mail: kliapi@mail.utexas.edu

Note. Discussion open until July 1, 2004. Separate discussions must be submitted for individual papers. To extend the closing date by one month, a written request must be filed with the ASCE Managing Editor. The manuscript for this paper was submitted for review and possible publication on February 8, 2002; approved on November 7, 2002. This paper is part of the ***Journal of Construction Engineering and Management***, Vol. 130, No. 1, February 1, 2004. ©ASCE, ISSN 0733-9364/2004/1-50–58/$18.00.

J. Constr. Eng. Manage., 2004, 130(1): 50-58

Fig. 1. Large scale manipulator mounted on crane

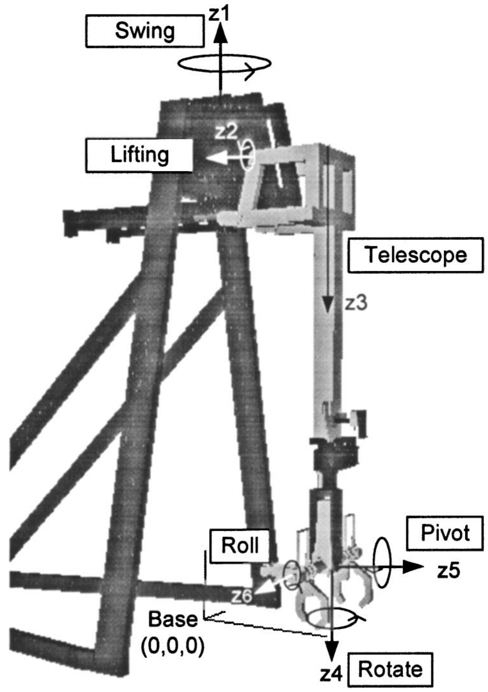

Fig. 2. Six degrees of freedom kinematic configuration for large scale manipulator

equipment feedback control. This general approach to error correction has been applied for many decades in the control of artillery fire, where error sources such as distance, wind direction, and air density are used by computer firing control programs to ''look up'' cross-hair adjustment factors in real time. The M1A1 battle tank works this way.

Objective and Methodology

The objective of the research presented here is to improve automated manipulator positioning capability based on regression modeling of manipulator position errors and causal factors. Causal factors of most interest are those that are most deterministic and numerically and easily measurable in real time so that the information can be used for control corrections. Causal factors may include temperature, humidity, payload, and other deterministic variables which may affect the accuracy of the manipulator.

The methodology pursued includes the following basic steps:

1. Select a set of well distributed known positions in the manipulator's working space;
2. Command the robotically controlled manipulator's end-point to the selected positions;
3. Measure actual positions of the resulting end-point and calculate position errors;
4. Repeat the above steps for variations of distance, hydraulic pressure, and payload;
5. Analyze the results using regression modeling; and
6. Develop an algorithm based on the regression modeling and apply the algorithm to adjust the commanded positions to reduce errors.

Kinematics

In order to obtain accurate position control, understanding the manipulator's link structure, sensory system (internal and external sensors), and control programs is necessary. Inverse and forward kinematics equations, computer algorithms, feedback encoders, and control interfaces were implemented for various control modes for the LSM in previous work (LeBlond et al. 1998). An illustration of the large-scale manipulator is shown in Fig. 2.

As seen in the figure, the LSM has swing, lift, telescope, rotate, roll, and pivot joints in total six degrees of freedom (DOF). Each joint and link pair can be associated with a coordinate frame, and each frame related via a standard transformation. Transformations are multiplied to relate series of frames, and based on what is called a ''back solve,'' the inverse kinematics can be used by the LSM control system to calculate a series of joint angles through which to move the joints in order for the end-effector frame to move from its initial location to its final location along a specified path. The transformation operator which is a 4×4 matrix is ''T'' (Craig 1989). Here, ${}^{\text{Base}}_{\text{Pivot}}T$ describes Pivot frame relative to Base frame and forms the following transform equation:

$$ {}^{\text{Base}}_{\text{Pivot}}T = {}^{\text{Base}}_{\text{Swing}}T \; {}^{\text{Swing}}_{\text{Lift}}T \; {}^{\text{Lift}}_{\text{Tele}}T \; {}^{\text{Tele}}_{\text{Rotate}}T \; {}^{\text{Rotate}}_{\text{Roll}}T \; {}^{\text{Roll}}_{\text{Pivot}}T \tag{2} $$

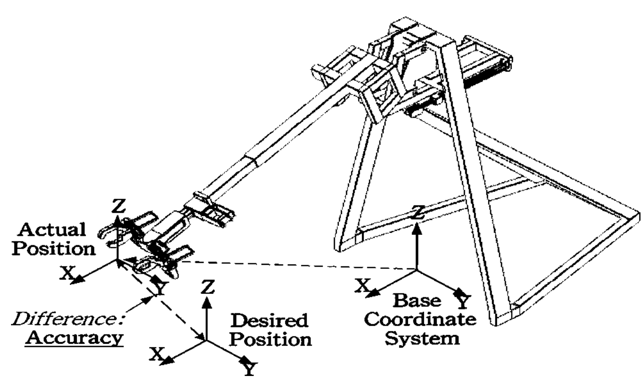

Fig. 3. Illustration of accuracy method relative to base coordinate system

J. Constr. Eng. Manage., 2004, 130(1): 50-58

Table 1. Chosen Kinematic States

	Kinematic states				Calculated global position of end-effector (cm)		
	Swing (°)	Lift (°)	Telescope (cm)	Rotate (°)	X	Y	Z
(1)	−20	11	0	20	158.00	−54.07	73.52
(2)	5	50	30.48	0	364.40	31.88	186.79
(3)	−10	36	60.96	0	321.09	−56.62	95.76
(4)	−2	31	16.76	−10	276.67	−11.30	112.23
(5)	10	21	0	0	216.26	38.13	95.52
(6)	0	54	48.77	0	393.93	0	197.40

Note: The values of roll and pivot joints are 0°.

For the LSM, these relationships are defined in detail and the inverse kinematics are solved for the rough terrain crane, field mounted manipulator configuration, and for the lab mounted configuration in Alciatore (1989) and Owen (1998), respectively.

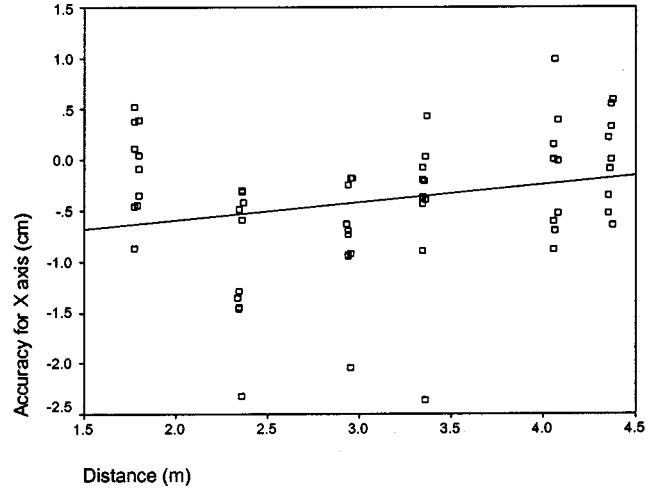

Fig. 4. Scatter chart for accuracy for X axis with respect to distance

Accuracy Tests

Accuracy is used here as an antonym for the definition of error used in the introduction. Either term is used for the same value depending on the context. Fig. 3 shows accuracy measurement relative to the manipulator's base coordinate system. On a construction site, the local positions of target objects relative to a mobile crane can be obtained in the Cartesian coordinate system of the operator or an automatic controller.

As another method, accuracy can be measured relative to a reference point within the manipulator's workspace. Wiersma (1995) explains that this accuracy method occurs when a specified output is planned from some reference point other than the base coordinate system. It is an especially important performance measure when working from a benchmark on a construction site. In this study, the accuracy was measured relative to the manipulator's base coordinate system without using a reference point.

In the following section, error source mechanisms are briefly discussed, the design of the data acquisition experiments is described, and the data is analyzed.

Error Source Mechanisms

Causal factors identified for this study are distance, payload, and hydraulic pressure (which are also used independent variables later). They work to produce error through mechanisms involving the manipulator's joints, and its deflection under load and extension of a boom. Random, nonsystematic sources of error are intermingled.

The joint errors of the LSM are mainly caused from stiction, backlash, and controller saturation which are influenced by mechanics and hydraulic pressure. The first two limit the minimum distances a joint can move from a stationary position to a new stationary position. Saturation limits the strength of the control signal that can be sent to an actuator (Owen 1998). Revolute joints tend to produce a larger error than prismatic joints because an angular error is multiplied by the link distance. Deflection increases as distance and payload increase and to some extent as hydraulic pressure decreases, since the hydraulic system volume is not perfectly fixed. Clearly error mechanisms interact in both canceling and augmenting fashions.

Table 2. Directional (Axial) Error Attributes with Respect to Distance

Axis	Regression model	n	r^2
X	$\Delta x = -0.962 + 0.180\,D_{\mathrm{istance}}$	60	0.059
Y	$\Delta y = 0.493 - 0.1\,D_{\mathrm{istance}}$	60	0.026
Z	$\Delta z = 0.0318 - 0.2411\,D_{\mathrm{istance}}$	60	0.122

Design of Experiments

To ensure a consistent test process, six different kinematic states of the LSM were chosen (Table 1). They were chosen to represent the full range of configuration that was anticipated to affect the various random error sources under the different conditions of the chosen three independent variables: distance, hydraulic pressure, and payload. Each kinematic state was tested under a range of payload (0, 40, 56, 112, and 386 kg) and hydraulic pressure (4,828, 6,207, 7,586, 8,966, and 10,345 kPa) conditions. This is a limited set for representing the full range of joint configurations, and it limits the ultimate usefulness of any regression result. It may be sufficient, however, to indicate whether a descriptive model or a regression model is feasible. If it is feasible, future

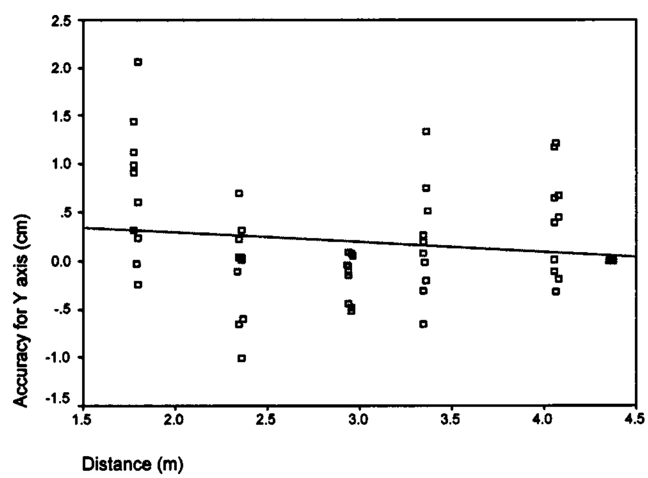

Fig. 5. Scatter chart for accuracy for Y axis with respect to distance

J. Constr. Eng. Manage., 2004, 130(1): 50-58

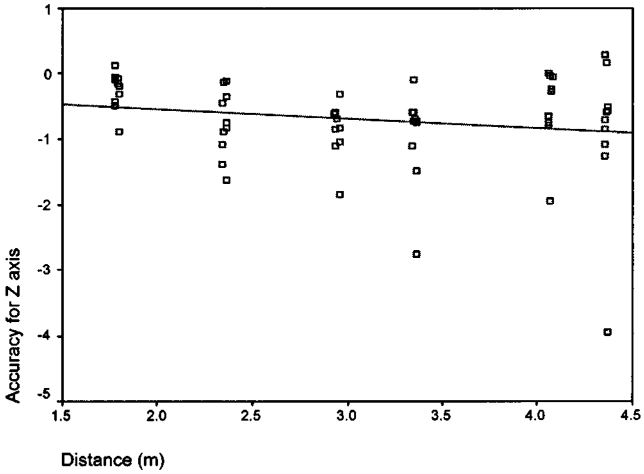

Fig. 6. Scatter chart for accuracy for *Z* axis with respect to distance

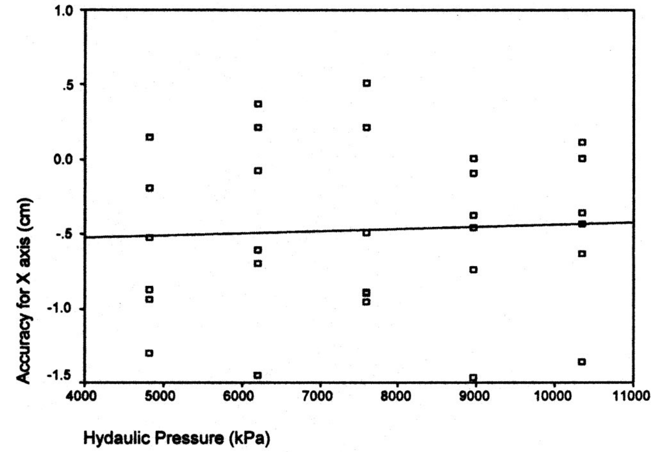

Fig. 7. Scatter chart for accuracy for *X* axis with respect to hydraulic pressure

studies may be conducted to more accurately and completely determine the relationship discovered.

Regression Analysis

There were two sets of experiments to collect data (e.g., pressure, payload). The sample (data) size was carefully selected which could be collected in one single day (about 15 h). Before this, measurement methods were developed over several weeks that could be proven to be accurate, reliable, and repeatable. This required many trial runs and preliminary test sets.

Accuracy with Respect to Distance

In this study, the distance is defined as the Cartesian positional difference between a base point (0,0,0) of the LSM's test bed and the kinematically calculated position (x,y,z) of the end-effector (e.g., $\sqrt{x^2+y^2+z^2}$). The accuracy test result for individual axial accuracies with signed values were tested by distances ranging from 0 to 4.5 m. Then the directional (axial) error attributes with respect to the distance variable were analyzed with collected sample data and the three equations were developed and summarized in Table 2 based on the found relationship between distance and each axial accuracy.

Here n indicates the sample size used and r^2 is called the coefficient of determination. Figs. 4, 5, and 6 show the scatter charts for accuracy, respectively, in each Cartesian dimension. Each regression line on the graphs indicates each axial equation shown in Table 2. As shown in Fig. 6, the conditional variance of accuracy in z coordinates increases while the distance increases, which is a behavior known as heteroscedasticity. The weighted least-squares (WLS) method was applied to correct for this behavior. Before correcting for heteroscedasicity, r^2 was 0.035. After the correction, r^2 increased to 0.122. Thus, distance had an effect on the directional error in the *Z* axis which would be expected. However, distance does not significantly affect the directional error in the *X* and *Y* axes; the coefficient of determination (r^2) for the x axis is 0.059 and for the *Y* axis is 0.026. Although distance does not significantly affect the position error attributes of the LSM when it is mounted on its frame inside the laboratory, common sense would seem to dictate that error in all dimensions would increase when the LSM is mounted on the crane as the crane's boom is extended to its full 25 m. While distance increased, the directional errors in the *Z* axis increased with a negative slope (Fig. 6), which is likely explained by deflection and hydraulic system volume expansion.

Accuracy with Respect to Hydraulic Pressure

As another variable for the regression analysis, hydraulic oil pressure was examined in order to find the error attributes of the LSM. Due to maintenance concerns, hydraulic pressure was limited to a maximum of 10,345 kPa (1,500 psi).

Table 3 and Figs. 7, 8, and 9 show the directional error attributes with respect to the hydraulic pressure. All the graphs indicate the error decreases toward zero while the hydraulic pressure increases.

Table 3. Directional (Axial) Error Attributes with Respect to Hydraulic Pressure

Axis	Regression model	n	r^2
X	$\Delta x=-0.58+0.00001412\,P_{\mathrm{ressure}}$	30	0.003
Y	$\Delta y=0.549-0.000043\,P_{\mathrm{ressure}}$	30	0.033
Z	$\Delta z=-1.29+0.00008942\,P_{\mathrm{ressure}}$	30	0.178

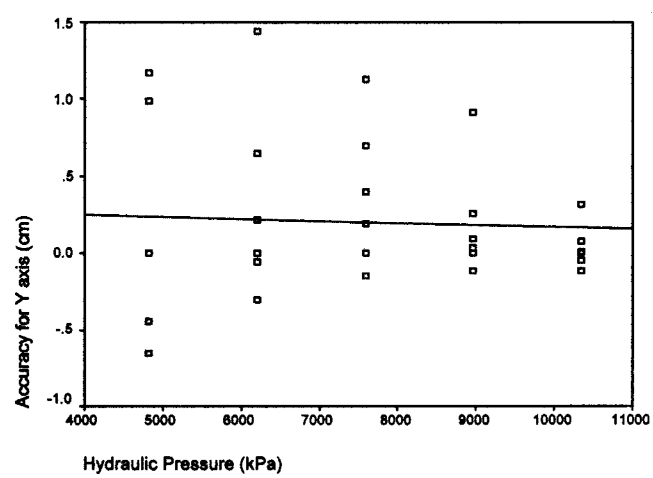

Fig. 8. Scatter chart for accuracy for *Y* axis with respect to hydraulic pressure

J. Constr. Eng. Manage., 2004, 130(1): 50-58

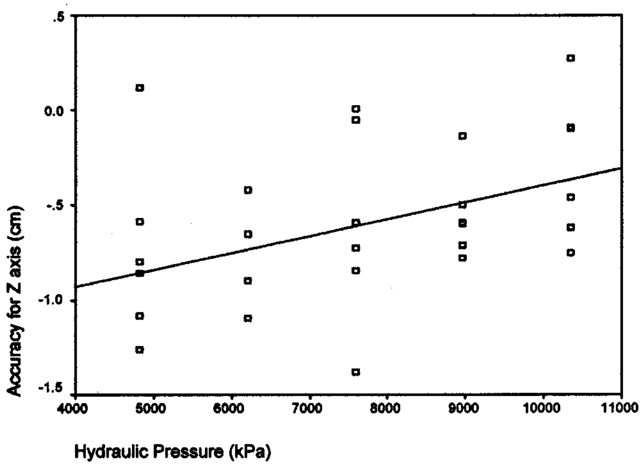

Fig. 9. Scatter chart for accuracy for *Z* axis with respect to hydraulic pressure

Similar to the previous accuracy test toward distance, hydraulic pressure showed some relationship with the directional error in the *Z* axis. The directional error in the *Z* axis decreased while hydraulic pressure increased. The increased hydraulic strength increases the joint speed, which might ultimately reduce the error caused from stiction and load. In a sense, the system is stiffer as well.

Accuracy with Respect to Payload

Payload does not include the weight of the end-effector or the arm, which are considered part of the manipulator (Wiersma 1995). Payload affects the inertia and speed of the manipulator, which can yield an overshoot error and more deflection, as described earlier. Four different pipes were used for this test (Fig. 10 and Table 4).

To ensure a consistent test process, the experiment was performed under 8,276 kPa (1,200 psi) of hydraulic pressure and six specific kinematic states of the LSM as previously described in Table 1. Each pipe was lifted into the chosen kinematic states of the LSM. Fig. 11 shows one of the chosen kinematic states.

Table 4. Properties of Pipes

	Name	Size (cm) Diameter×Length	Weight (kg)
1	Aluminum/concrete pipe	15.24*D* × 124.46*L*	39.7345
2	Aluminum/concrete pipe	15.24*D* × 172.72*L*	55.6555
3	Aluminum/concrete pipe	20.32*D* × 172.72*L*	111.9460
4	Steel/concrete pipe	27.94*D* × 152.4*L*	385.5515

Note: *D*=diameter; *L*=length.

The directional (axial) error attributes with respect to the payload variable were analyzed and summarized in Table 5.

Figs. 12, 13, and 14 show scatter diagrams for accuracy, respectively, in each Cartesian dimension. The coefficient of determination r^2 for the *X* axis (0.507) and the *Z* axis (0.531) and their regression line slopes in the scatter charts indicate that the payload significantly affects the accuracy of the *X* axis and the *Z* axis. It is clear that payload accentuates the deflection which explains the increased error in *z* coordinates. In addition, payload makes the LSM move sluggish which might cause in more errors toward the *X* axis which has a 4.6 m range than toward the *Y* axis which has 2.2 m range. In addition, the lift joint and the telescope joint which determine most of *x* and *z* coordinates relatively are slower than the swing joint which determines most of *y* coordinates. Payload makes the lifting and telescoping motions more sluggish, which might ultimately cause some systematic relationship with errors in *x* and *z* coordinates. Also, *x* and *z* coordinates relate to degree of cantilever and therefore deflection.

As shown in Figs. 13 and 14, the conditional variances of accuracy in *y* and *z* coordinates conditional upon the given payload, increase while the payload increases with systematic patterns (heteroscedasticity); it could be caused by randomly integrated several error sources affected by heavier load such as stiction, overshoot, and deflection. Most probably it reflects the fact that the variances of accuracy increase as the arm is extended or as moment about the lift joint increases.

Although there was almost no relationship between payload and the directional error in the *Y* axis, the systematically increased conditional variance of accuracy in the *Y* axis might be caused from erratically applied error sources such as stiction and overshoot to the swing joint. Especially, the swing joint which determines that most of *y* coordinates has a relatively faster motion

Fig. 10. Pipes for payload test

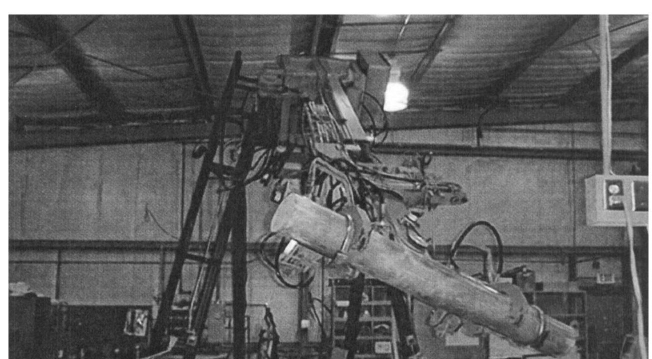

Fig. 11. One of chosen kinematic states

J. Constr. Eng. Manage., 2004, 130(1): 50-58

Table 5. Directional (Axial) Error Attributes with Respect to Payload

Axis	Regression model	n	r^2
X	$\Delta x = 0.151 - 0.00397\, P_{\text{ayload}}$	30	0.507
Y	$\Delta y = 0.124 + 0.0002431\, P_{\text{ayload}}$	30	0.003
Z	$\Delta z = -0.267 - 0.00459\, P_{\text{ayload}}$	30	0.531

than other joints; so it could cause an overshoot error with increased inertia as an object's inertia is determined by its mass. On the contrary, increased payload might increase stiction as well. This might explain why the variances spread out around zero as shown in Fig. 13.

However, the transformed data by the weighted least square (WLS) method indicates the lower coefficient of determination r^2 in both the y and z coordinates (y: 0.0027 and z: 0.251). Furthermore, the transformed data by the log transformation method did not improve the regression model (r^2 was 0.008 for the Y axis and 0.459 for the Z axis). It explains that the transformation of the original model by the WLS and the log transformation processes do not improve the result (r^2); they do not reduce the estimated standard errors. Thus, the original model was kept without modification.

Integrated Error Modeling

The error modeling for the large-scale manipulator is nontrivial. Even though payload is the most significant error-producing factor in this application, there are other, related, significant factors which can accentuate or attenuate position errors (such as mass distribution, orientation, and center of gravity).

While performing error tests, only one configuration (the fifth row from the top in Table 1) repeatedly yielded a relatively larger error than the average errors of the other configurations under the same other conditions. This implies that there are some other factors which accentuate position errors in certain orientations.

Even though orientation and mass distribution may not be easily used as numerical variables in regression modeling, they were statistically involved in the error modeling results. In other words, this approach incorporated such random error components based on load, distance, and hydraulic pressure.

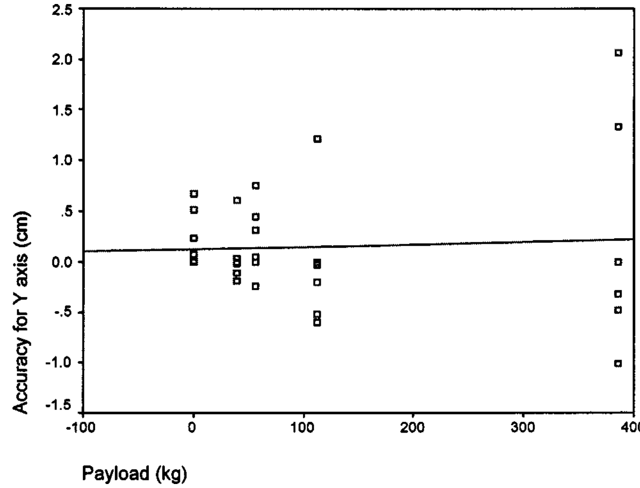

Fig. 13. Scatter chart for accuracy for Y axis with respect to payload

Error Adjustment with Multivariable Regression Models

The multivariable regression analysis of the LSM's position with respect to distance, hydraulic oil pressure, and payload can be modeled as follows:

$$\Delta_{\text{error}} = \hat{\beta}_0 + \hat{\beta}_1 D_{\text{istance}} + \hat{\beta}_2 P_{\text{ressure}} + \hat{\beta}_3 P_{\text{ayload}} \tag{3}$$

Here $\hat{\beta}_0$, $\hat{\beta}_1$, $\hat{\beta}_2$, and $\hat{\beta}_3$ indicate coefficients for a sample regression equation. To adjust the LSM's positional error based on the sample data, the error of each axis of the end-effector was analyzed with the multivariable model.

1. Regression of the multivariable model on the LSM's X axis position error (ΔX)

$$\Delta X = -1.229 + 0.182 D_{\text{istance}} + 0.0000528 P_{\text{ressure}} - 0.00264 P_{\text{ayload}}, \quad (r^2 = 0.262) \tag{4}$$

Regression of the multivariable model on the LSM's Y axis position error (ΔY)

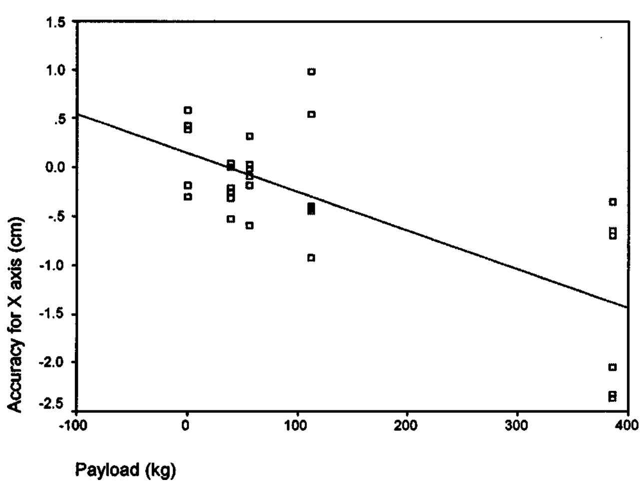

Fig. 12. Scatter chart for accuracy for X axis with respect to payload

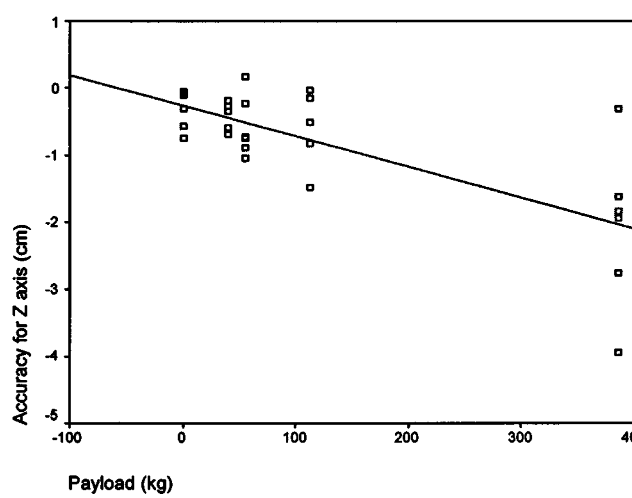

Fig. 14. Scatter chart for accuracy for Z axis with respect to payload

J. Constr. Eng. Manage., 2004, 130(1): 50-58

Table 6. Axial Error Adjustment for Test Data Set

Average accuracy	X	Y	Z	Total accuracy
Before adjusted (cm)	0.5731	0.3859	0.7309	1.1717
After adjusted (cm)	0.4649	0.4009	0.3614	0.8115
Percent reduced	18.88	−3.66	50.55	30.74

$$\Delta Y = 0.627 - 0.1D_{\text{istance}} - 0.000018P_{\text{ressure}} + 0.0000988P_{\text{ayload}}, \quad (r^2 = 0.028) \tag{5}$$

Regression of the multivariable model on the LSM's Z axis position error (ΔZ)

$$\Delta Z = -0.884 - 0.141D_{\text{istance}} - 0.0001075P_{\text{ressure}} - 0.00397P_{\text{ayload}}, \quad (r^2 = 0.483) \tag{6}$$

Unlike electrically operated manufacturing robots which have high accuracy, hydraulically operated heavy manipulators do not exhibit well-behaved systematic biases because they are combined with random error sources such as stiction that cause the variance to be significant and the r^2 values to be limited as shown Eqs. (4), (5), and (6).

By applying the statistical multivariable equations to the same data set obtained from the LSM's position accuracy test, given the three conditional variables, there were some error reductions (30.7%) in the overall accuracy shown in Table 6. Fig. 15 shows how Table 6 developed. In a theory, the substantial number of the unsolved errors (69.3%) may be statistically solved by adding more conditional variables.

While the average errors of the X axis and the Z axis were reduced by 18.88 and 50.55%, respectively, the average error of the Y axis increased by using the multivariable equations. This means that the multivariable equation [Eq. (5)] does not explain the Y axis errors very well. Also, it can be inferred from Eq. (5) in which r^2 is 0.028, that the multiple variables have little effect on the Y axis accuracy. Therefore, while adjusting the X and Z axis values based on Eqs. (4) and (6), the kinematically calculated original Y axis value was not adjusted.

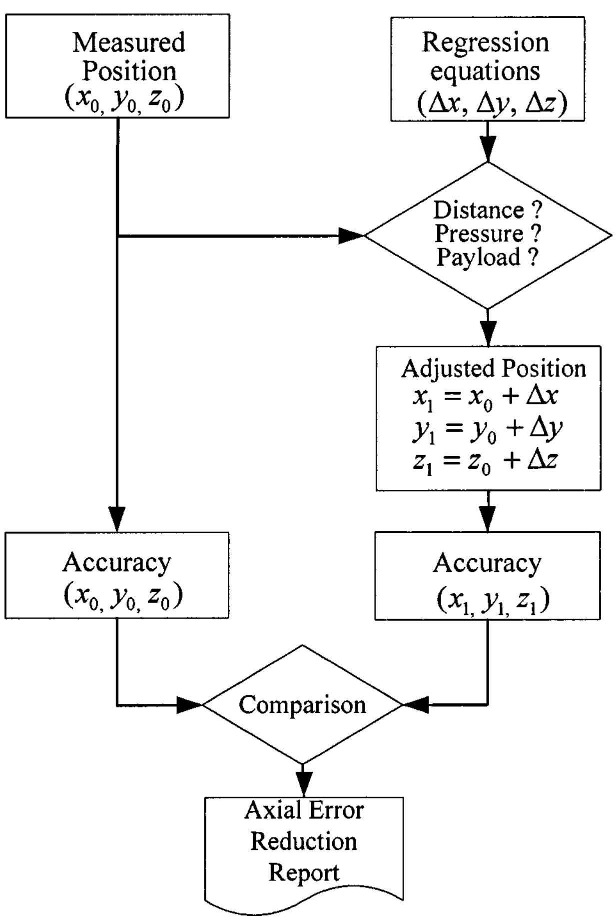

Fig. 15. Accuracy comparison process

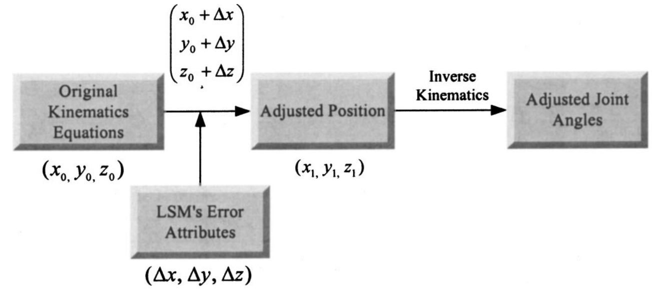

Fig. 16. Kinematics position data adjustment process

Final Performance Tests

The obtained three equations were then applied to the original forward kinematics equations to adjust for the original x-y-z coordinates. Then, the inverse kinematics provides adjusted six joints angles based on the adjusted position data. Fig. 16 illustrates this process.

To verify the error attributes found from the error modeling tests, several material placement tests were conducted on the LSM's test bed. First, a stylus was attached to the test load (386 kg) in the LSM's jaws pointing toward a target. By using a laser rangefinder, a Cartesian coordinates of a center of cross hairs on a target plane was measured (325.62, 10.77, and 77.10 cm). Based on the six joint values obtained from inverse kinematics, then the

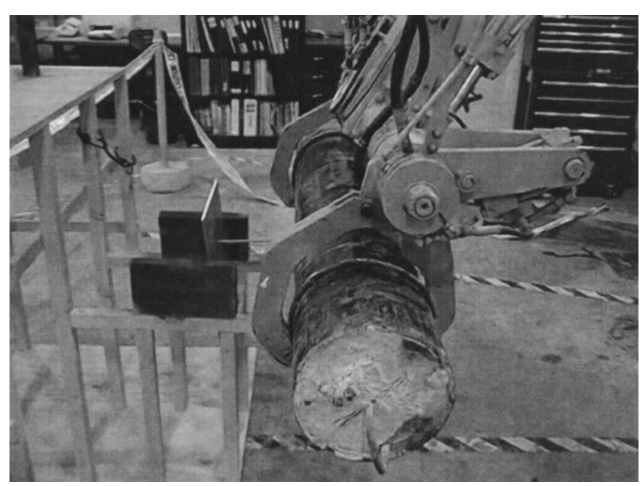

Fig. 17. Accuracy test with stylus and test load

J. Constr. Eng. Manage., 2004, 130(1): 50-58

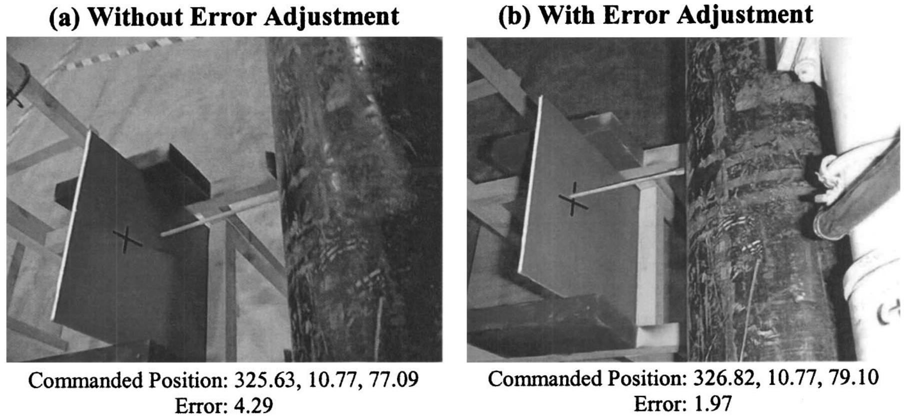

Fig. 18. Large scale manipulator accuracy test result comparison (unit: cm)

stylus was moved toward the target point by operating the LSM (see Fig. 17). The purpose of this test was to compare the LSM's accuracy when its error was adjusted and unadjusted under a certain working condition (with 3.348 m distance, a 386 kg test load, and a 8,276 kPa hydraulic pressure supply). The working condition was then applied to Eqs. (4) and (6) to adjust errors in X and Z axis, respectively, as follows:

$$\Delta X = -1.229 + 0.182 \times 3.348 \text{ m} + 0.0000528 \times 8276 \text{ kPa} - 0.00264 \times 386 \text{ kg} = 1.2 \text{ cm [Eq. (4)]}$$

$$\Delta Z = -0.884 - 0.141 \times 3.348 \text{ m} + 0.0001075 \times 8276 \text{ kPa} - 0.00397 \times 386 \text{ kg} = 2.0 \text{ cm [Eq. (6)]}$$

Then the calculated values were added to the original position measurement (325.62+1.2 cm, 10.77 cm, and 77.10+2.0 cm), and the manipulator was commanded to move to the modified position. A test result shows that the LSM has better accuracy when a commanded position was modified based on the developed error modeling (see Fig. 18).

The aforementioned error adjustment process could be easily conducted in the real-time manner by using the user interface programmed in *Visual Basic* (Fig. 19). As an external sensor, a laser rangefinder mounted on the LSM was used to measure the target position (Cho et al. 2002). According to the LSM's joint values and external sensors' values, the user interface calculated the target position based on the programmed forward kinematics. Then, the LSM's operation condition inputs were used to adjust the error. Finally, the user interface shows the x-y-z adjusted target position.

The other tests included a horizontal placement of a wooden beam and an aluminum pipe and vertical placements of aluminum pipes on a pipe rack (see Fig. 20). Positions on the target material surface and on the pipe rack were obtained by a laser rangefinder mounted on the LSM. Based on the error modeling results, each position measurement was adjusted for to reduce magnitude of possible errors by reflecting upon the three variables—distance, hydraulic pressure, and payload. The material placement test was successfully performed without any collision between objects.

Conclusion

The error attributes of a hydraulically actuated large scale manipulator were analyzed by using regression analysis. In the regression analysis, three variables, distance, hydraulic pressure, and payload, were individually varied to find the position error attributes of the LSM. Distance had a somewhat significant effect on the directional error in the Z axis (as distance increased, random errors in the Z axis increased). Hydraulic pressure and payload had a significant effect on the overall error (as hydraulic pressure decreased and payload increased, random error increased). Although the testing was performed in a small working volume due to the limited mobility of the LSM on its fixed frame, this study reduced about 30% of the average positioning errors of the LSM with an integrated multivariable regression model. Thus, it is sufficient to indicate whether a descriptive model or a regression model is feasible. The substantial number of the unsolved errors (about 70%) may be statistically solved by adding more conditional variables which possibly affect the manipulator's position errors. Therefore, the error modeling tests performed in this research can be used by engineers in their current state or can be modified to improve the accuracy and precision of control systems of automated and semiautomated construction equipment such as back-hoes, concrete pumps, and cranes. Manufacturers such as Caterpillar, Komatsu, and Trimble/Spectra-Physics are working actively in this area and offering new products that could be enhanced using the results presented here.

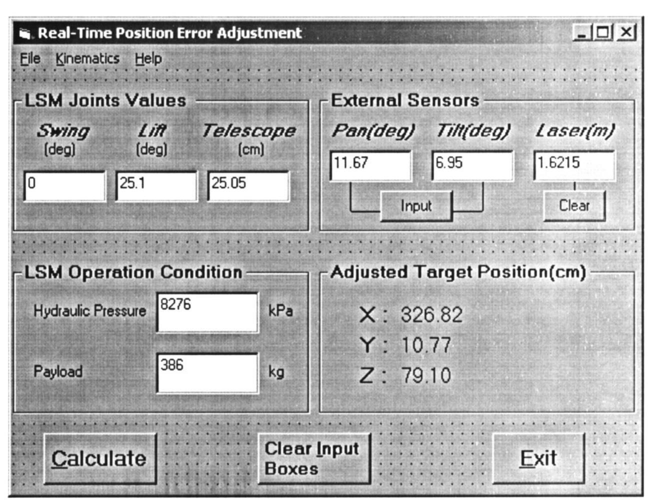

Fig. 19. Real-time position error adjustment user interface

J. Constr. Eng. Manage., 2004, 130(1): 50-58

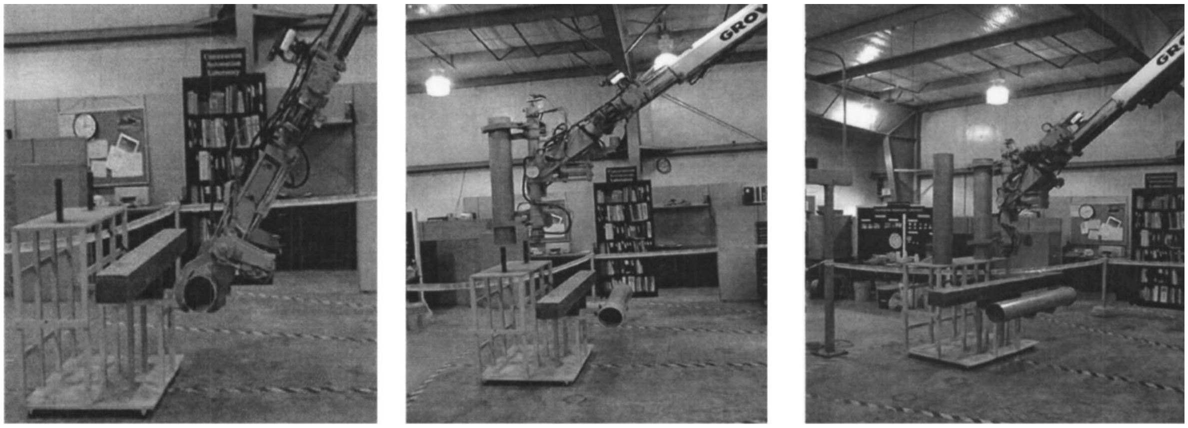

Fig. 20. Materials placement test on pipe rack

Future Study

Although the error modeling test method developed in this study proved to be feasible, the testing is so far of a preliminary nature, as more exhaustive tests need to be run on a wider range of working conditions and system configuration to more accurately and completely determine the relationship among error sources discovered.

Other variables, such as humidity, temperature, human error, orientation, and mass distribution, may also be considered to find their effects on the LSM's error attributes. More variables and bigger sample sizes may provide a more reliable error model. These were not performed in this study due to the complexity involved and to control limitations of the work environment. Also future studies may include an accuracy confidence modeling indicating sizes of envelops of confidence for accuracy at each state of the LSM configurations based on each working condition (causal factor).

Acknowledgments

This paper is based on the research funded by National Science Foundation (Grant No. CMS-0000137). The writers gratefully acknowledge their financial support and encouragement throughout this study.

References

Alciatore, D. (1989). ''Automation of a piping construction manipulator and development of a heuristic application-specific path planner.'' PhD dissertation, Dept. of Civil Engineering, The Univ. of Texas at Austin, Tex.

Cho, Y., Haas, C., Sreenivasan, S., and Liapi, K. (2002). ''A framework for rapid local area modeling for construction automation.'' *J. Autom. Const.*, 11(6), 629–641.

Craig, J. (1986). *Introduction to robotics: Mechanics & control*, Addison-Wesley, Reading, Mass., 35–39.

Huang, X., and Bernold, L. E. (1997). ''CAD integrated excavation and pipe laying.'' *J. Constr. Eng. Manage.*, 123(3), 318–323.

LeBlond, D., Owen, F., Gibson, G., Haas, C., and Traver, A. (1998). ''Control improvement for advanced construction equipment.'' *J. Constr. Eng. Manage.*, 124(4), 289–296.

Owen, F. C. (1998). ''Development of smooth resolved motion and computer-assisted teleoperation for a large scale manipulator.'' PhD dissertation, Dept. of Mechanical Engineering, The Univ. of Texas at Austin, Tex.

Papanikolopoulos, N., and Smith, C. E. (1998). ''Issues and experimental results in vision-guided robotic grasping of static or moving objects.'' *Ind. Robot*, 25(2), 134–140.

Singh, S. (1997). ''The state of art in automation of earthmoving.'' *J. Aerosp. Eng.*, 10(4), 179–188.

Wiersma, M. E. (1995). ''Standards and benchmark tests for evaluating large scale manipulators with construction applications.'' Master's thesis, Dept. of Mechanical Engineering, The Univ. of Texas at Austin, Tex.

J. Constr. Eng. Manage., 2004, 130(1): 50-58